Advances in Concrete Construction, *Vol. 8, No. 1 (2019) 9-19*
DOI: https://doi.org/10.12989/acc.2019.8.1.009

Damage evaluation of RC beams strengthened with hybrid fibers

Radhika Sridhar* and Ravi Prasad[a]

Department of Civil Engineering, National Institute of Technology, Warangal, India

(Received August 17, 2018, Revised April 5, 2019, Accepted April 9, 2019)

Abstract. This paper describes an experimental investigation on hybrid fiber reinforced concrete (HYFRC) beams. And the main aim of this present paper is to examine the dynamic characteristics and damage evaluation of undamaged and damaged HYFRC beams under free-free constraints. In this experimental work, totally four RC beams were cast and analyzed in order to evaluate the dynamic behavior as well as static load behavior of HYFRCs. Hybrid fiber reinforced concrete beams have been cast by incorporating two different fibers such as steel and polypropylene (PP). Damage of HYFRC beams was obtained by cracking of concrete for one of the beams in each set under four-point bending tests with different percentage variation of damage levels as 50%, 70% and 90% of maximum ultimate load. And the main dynamic characteristics such as damping, fundamental natural frequencies, mode shapes and frequency response function at each and every damage level has been assessed by means of non-destructive technique (NDT) with hammer excitation. The fundamental natural frequency and damping values obtained through dynamic tests for HYFRC beams were compared with control (reference) RC beam at each level of damage which has been acquired through static tests. The static experimental test results emphasize that the HYFRC beam has attained higher ultimate load as compared with control reinforced concrete beam.

Keywords: composite materials; compressive strength; fiber-reinforced concrete; non-destructive testing; vibration

1. Introduction

Damage assessment plays an important role in the evaluation of the stability and strength of structure, which is significant for both the existing ones and those under construction, Barros and Dias (2006). Reinforced concrete structures may also be subjected to damage as a result of insufficient reinforcement, large deflection and poor quality of concrete, corrosion of steel reinforcement or insufficient capacity, Haung (2010). In the last decades, structural health monitoring has undergone facilitation with enormous applications on civil constructions such as bridges, towers, frames and beams and in new, vibration researches also, Huzsav (2008). The flexibility to assess any concrete structure and perceive damage in its earliest state could be easily done or achieved only through vibration analysis method, Capozzuca (2009). The essential concept concealed with vibration monitoring technique for any reinforced concrete structure damage analysis would be based on dynamic characteristics and does not rely on the geometry of the structure; as a result, changes will occur in the dynamic response behavior, Capozzuca (2013).

Besides, vibration based monitoring technique; many methods have been reported in literature to analyze the damage, Caleb *et al*. (2009) such as change in modal strain energy method, change in flexible method and structural model updated method, Capozzuca (2018). Constatine *et al*. (2016) studied the damage evaluation of reinforced concrete beam using piezoelectric sensors through the application of wireless admittance monitoring system by exploitation of monotonic and cyclic loading conditions. Eventually, thedamage of reinforced concrete beam has been quantified through the discrepancies between the frequency response of the undamaged and the scrutinized damage levels. Acoustic emission is a non-destructive technique (NDT) which has been used for both the identification of damage level and the nature of damage in reinforced concrete beam which keeps the structure in safety condition, Shahiron *et al*. (2013). Dynamic properties of reinforced concrete slab has been assessed by vibration based method which is one of the most promising technique of NDT with hammer excitation which could identify the damage in reinforced concrete specimen with the changes in natural frequencies, Hamed *et al*. (2018). The main dynamic properties of structural materials such as mass, stiffness, damping, fundamental frequency, mode shape and amplitude of excited force would give the dynamic behavior of any structure, Capozzuca *et al*. (2016).

Concrete is a composite material which is extensively used in recent years since it has several specific advantages such as economical, hardened at ambient temperature, ability to cast into shape and has ability to consume and recycled, Brandt (2008). Generally concrete is classified as a brittle material; however reinforced concrete with short fibers distributed randomly would improve the strength of the cementitious matrices by controlling the initiation, propagation and merging of cracks, Lim and Ozbakkaloglu (2014). There has been a great density of materials used for this purpose such as carbon, steel, polypropylene, glass, and natural fibers, Alberti *et al*. (2014). Among these materials, steel and some non-metallic fibers which have been used in

*Corresponding author, Research Scholar
E-mail: radhi.kalasridhar@gmail.com
[a]Ph.D. Student

ISSN: 2287-5301 (Print), 2287-531X (Online)

Table 1 Physical and mechanical properties of steel and PP fibers

Type of fibers	Shape of fibers	Length (mm)	Diameter (mm)	Aspect ratio	Tensile strength (MPa)	Modulus of elasticity (GPa)	Density (kg/m^3)	% of elongation
Steel	Hooked end	35	0.5	70	1100	210	7850	2
PP	Straight	12	0.038	315	420	5	990	11

Fig. 1 Typical view of steel fiber

Fig. 2 Typical view of polypropylene fiber

concrete to improve the mechanical properties and the combination of the fibers may also be taken into account in the structural design forming a new composite material called as hybrid fiber reinforced concrete, Muntean *et al*. (2017). The most commonly used fiber is steel fibers because of their high tensile strength and greater modulus of elasticity, Di Prisco *et al*. (2008). In the recent years, recycled steel fibers have been used in concrete for the potential utilization as well as a substitute for the fibers which improves the fracture resistance of the concrete when compared with commercial steel fibers, Filip *et al*. (2019). Chaohua *et al*. (2014) studied the combination of chopped basalt fibers under tensile behavior which concluded that the contribution of energy absorption capacity of the concrete is mainly due to the role of percentage combination of fibers when compared with non-fibrous concrete. Renewable source like bamboo has been used for reinforcing the concrete which is simple, efficient and economical for rural construction which enhances the mechanical performance of concrete as well as ultimate load of the member, Ganesan *et al*. (2018).

Despite steel fibers are the most extensively used material in concrete for reinforcement purpose, in the last decade, an inventive solutions obtained by combining different types of fibers and cementitious materials are getting more recurrent, Tiberti (2014). They are predominantly mentioned as hybrid fiber reinforced concrete and their behavior was specially investigated with the aim of understanding the possible synergetic action of fibers in order to enhance the post cracking strength or response of the structure, Naaman and Reinhardt (2006). Applications in the field are based on employing hybrid fibers in the same structure, such as polypropylene hybrid fiber reinforced concrete including staple and monofilament fibers, macro and micro steel fibers, twisted macro and hooked-end fibers and short and long hooked-end steel fibers, Kim *et al*. (2011). A structure which is reinforced with two or more hybrid fibers such one metallic and two non-metallic fibers and two metallic and one non-metallic fibers to provide condescending properties of the same structure, Dawood and Ramli (2010). Shaikh and Taweel (2015) has also been studied that the addition of hybrid fibers such as steel and basalt in concrete reduces the spalling and explosive failure of reinforced concrete beam after exposed to elevated temperature of 800 degree Celsius. Some cracks occur at different stages and sizes in concrete, the use of various fibers with different lengths are a better way to rectify the problem, Yao eta al (2003). The main purpose of the combination of different types of fibers is to control both micro and macro cracks at different zones of the cementitious material, at different damage levels and during different impact loading or dynamic loading conditions, Yang (2011).

1.1 Research significance

Although, significantly more literature is needed that addresses the enormous and various conditions that are inherent in applying vibration monitoring technique to the assessment of structural integrity of any reinforced concrete beams strengthened with fiber reinforced concrete. Based on the aforementioned affirms, an experimental program has been developed to evaluate the damage assessment of hybrid fiber reinforced concrete beams under dynamic tests. The experimental research was developed with large-scale modeling of HYFRC beams, totally four reinforced concrete (RC) beams have been cast by incorporating hybrid fibers including control RC beams to acquire the objective as well as to compare.

2. Experimental program

The damage assessment of hybrid fiber reinforced concrete beam incorporating steel and polypropylene fibers has been developed and studied under static and dynamic load tests.

2.1 Basic constituents of materials

Ordinary Portland cement (OPC) of 53 grade cement according to Indian Standard code was used in this present

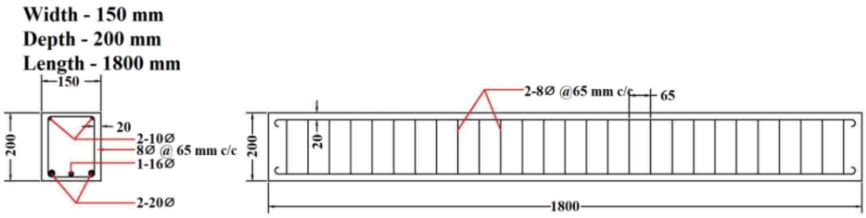

Fig. 3 Detailing of RC beam

Fig. 4 Pre-fabricated reinforcement cages

study which has a specific gravity of 3.15 and a bulk density of 1140 kg/m^3. On further, this cement has a recorded compressive strength of 53.5 MPa at the age of 28 days.

Fly-ash was added along with cement at approximately 12% by its mass in order to attain the desired strength of M50 grade concrete and also for the ease dispersion of fibers. Coarse aggregates with the maximum and minimum sizes of 20 mm and 10mm with a 6.34 fineness modulus was used. Locally available river sand having a fineness modulus of 2.86 has been used as fine aggregates. Tap water mixed with super-plasticizers was used to mix the ingredients in order to increase the workability of the mixture. The hybrid fiber reinforced concrete composites were prepared using different fiber volume fractions with different percentage variations of steel and PP fibers in this present work and only one mixture with total fiber volume fraction as 0.5% has been chosen for casting HYFRCs. The steel fibers used in this present investigation were hooked-end whilst polypropylene (PP) fibers were straight. The aspect ratio of PP and steel fibers used in this research work are 70 and 315 respectively. The steel and PP fibers were produced from locally available market. The physical and mechanical properties of steel and PP fibers are tabulated in Table 1. Fig. 1 and Fig. 2 show the typical view of steel and polypropylene fibers used in this study.

2.2 Fabrication of specimens

In this experimental investigation, totally four reinforced concrete beams were fabricated and cast. All specimens were initially designed as 1800 mm long with a rectangular cross-section of 150 mm wide and 200 mm deep. All beams have been designed as under-reinforced section based on the area of tensile reinforcement to prevent the catastrophic failure of the structure. Each beam has been reinforced with high-tensile strength bars of Fe500 and the detailing of RC beam is shown in Fig 3. Fig. 4 displays the pre-fabricated reinforcement cages. Among four RC beams, two beams were cast for static load tests in order to examine the

Table 2 Designation of RC beam specimens

Mixture series	Beam designation	Beam type	Type of test
1	M50Control-S (B_1)	RC	Static
2	M50Control-D (B_2)	RC	Dynamic
3	M50Hybrid-S (P_1)	HYFRC	Static
4	M50Hybrid-D (P_2)	HYFRC	Dynamic

damage evaluation under dynamic tests of the rest beams in terms of percentage variation of damage degrees as D_0, D_1, D_2 and D_3. Designations of HYFRC and control RC beams are illustrated in Table 2.

2.3 Mixing, casting and curing procedures

The concrete mix design was prepared according to Indian Standard code for concrete mix design which is based on the technical properties of the material. The mixing process started with the dry mixing of the coarse and fine aggregates for one minute. The cement mixed with fly-ash was added and it was kept for another one minute. Then steel fibers were added to the mixture and again it was continued for another two minutes till the fibers were dispersed properly to concrete. Water mixed with super-plasticizers was added and mixed for another 2 minutes.

After the former process, polypropylene fibers were added to the wet concrete and the mixture was mixed for another 3 minutes to ensure that the fibers can evenly disperse throughout the concrete. Then the fresh concrete was cast in steel molds such as cubes, cylinders and prisms and was compacted on a vibration table. All specimens were demolded after 24hrs and then were immersed in water at room temperature of 28° C until their 28 days testing ages. Mix proportion of plain and hybrid fiber reinforced concrete for M50 grade is tabulated in Table 3. Fig 5 displays the casting of reinforced concrete beams.

2.4 Mechanical property test procedures

To evaluate the composite performance of hybrid fiber

(a) Steel molds for RC beam with reinforcement

(b) Casting of RC beams

Fig. 5 Preparation sequence of RC beams

Table 3 Mix proportions of plain and HYFRCs

Mix No	Mixture name	Cement	Fly-ash	Fine aggregate	Coarse aggregate	W/C ratio	Super-Plasticizers (%)	Total V_f (%)	Steel Fibers (%)	PP Fibers (%)
1	M50C	1	0.12	1.56	2.94	0.31	0.3	0	0	0
2	M50HY	1	0.12	1.56	2.94	0.31	0.3	0.5	75	25

* Note: Content of steel and PP fibers are expressed as total volume fraction of concrete, while all the other ingredients are expressed as unit weight proportions of cement content.

Table 4 Mechanical property test results of plain and HYFRCs

Mix No	Mixture name	Compressive strength (MPa)	Splitting tensile strength (MPa)	Flexural strength (MPa)
1	M50C	57.53	4.36	5.38
2	M50HY	63.56	6.84	8.87

Table 5 Static test results of RC and HYFRC beams

Mix No	Beam designation	Ultimate load (kN)	% Increase of load
1	M50Control-S (B_1)	208.5	-
2	M50Hybrid-S (P_1)	248	18.94

reinforced concrete, three cubes and cylinders of standard size (150 mm×150 mm×150 mm) and (150 mm diameter and 300 mm height) respectively, for each mixture were cast and tested in universal compression testing machine of 3000 kN capacity after 28 days of its curing period in accordance with bureau of Indian standard code.

In order to determine the flexural properties of plain and hybrid fiber reinforced concrete, 4 point bending flexural test was carried out. The beam of size (500 mm×100 mm×100 mm) was used in this study. The mid-span length of 133.33 mm is one-third of the simply supported clear span length of 400 mm and the support span of the four point bending test set up is of 50 mm. All specimens were tested under a dynamic universal testing machine with a capacity of 1000 kN and specimens were loaded until complete failure under displacement control at a loading rate of 0.20 mm/min.

2.5 Flexural load tests of RC beams

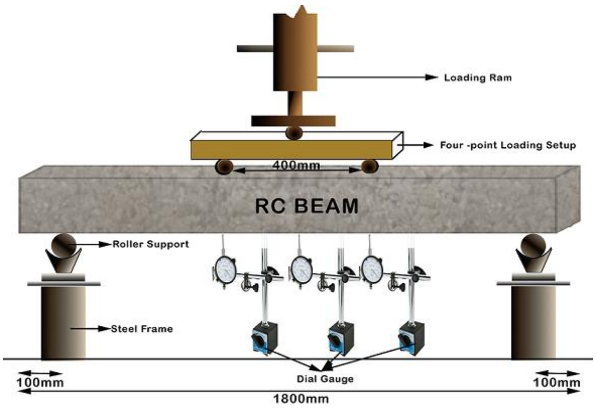

Fig. 6 Schematic view of static load test setup

In this experimental investigation, all beams were tested under universal testing machine of 3000 kN capacity to evaluate the ultimate flexural load and maximum moment of control RC beams and HYFRC beams. The beam specimens were placed on the steel support with rollers on each end and the load was applied through four-point loading system. Three dial gauges were used in the present experimental investigation in order to determine the central and overall deflection of the beam at each and every loading point. The schematic view of static load test setup is shown in Fig. 6.

2.6 Flexural load tests of RC beams

Modal test was performed on both damaged and undamaged beams using a transfer function technique in free-free constraints. The accelerometer has been placed on the specimen at one particular node to collect the response

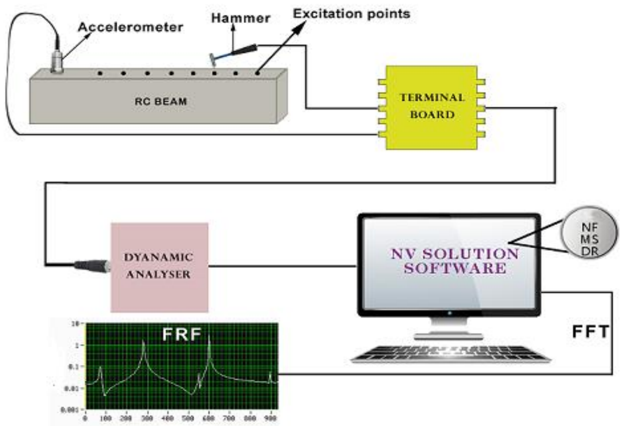

Fig. 7 schematic view of modal test setup

Fig. 8 Failure pattern of prismatic beam

Fig. 9 Typical view of static load test setup

while vibrating the structure. The modal analysis was carried out using dynamic analyzer in this study. It consists of an input as well as output device.

There will be a central unit which receives the signal from the input device and sends to the computer for further analysis. All the data will be stored in the computer which can be retrieved in any form as per the requirements. The Frequency Response Function (FRF) obtained from dynamic analyzer was fed into smart office-NV solution to obtain the required output.

All the specimens were tested in free-free condition by keeping the accelerometer at one constant node which was fixed and the specimens were excited using an impact hammer at any point and the corresponding FRF was recorded at that point in order to evaluate the natural frequency for damage assessment. The aforementioned procedure has been repeated for all other points without moving the accelerometer from the initial point and this method is referred as roving impact hammer method. A channel analyzer was used to acquire the signals and to

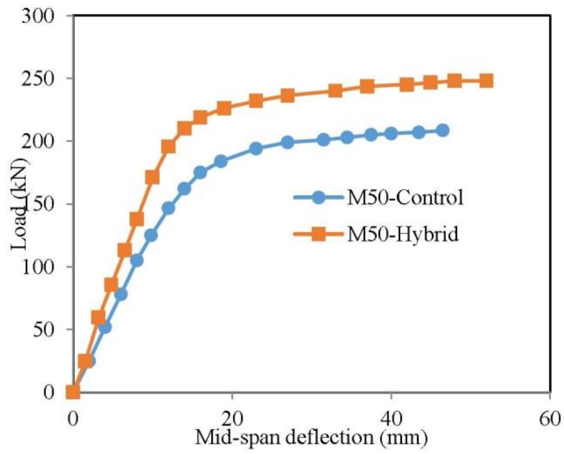

Fig. 10 Load Vs. Mid-span deflection of control RC and HYFRC beams

obtain the frequency response function (FRF) from the response and the excitation force through the hammer. Fig. 7 depicts the schematic view of modal test setup. Modal parameters such as natural frequency, damping ratio and mode shape were extracted through the modal analysis software. Also, the modal test was performed for all beams at the end of each damage degree as D_0 (undamaged condition), D_1 (50% of ultimate load), D_2 (70% of ultimate load) and D_3 (90% of ultimate load) in order to evaluate the damage behavior of control RC and HYFRC beams.

3. Results and discussion

Main results obtained by experimental tests are shown and discussed in this chapter. Static results define the behavior of control RC and HYFRC beams and the dynamic results reveal the knowledge of dynamic response behavior on damaged and undamaged states.

3.1 Mechanical property tests

The acquired test results of compressive, flexural and split-tensile strength are summarized in Table 4. Furthermore, failure pattern of prismatic specimen is shown in Fig. 8. Each magnitude of strength has shown in table is a mean of three specimens tested in the laboratory after proper curing period. HYFRC specimen incorporated with 75% of steel fibers and 25% of PP fibers with a total volume fraction of 0.5% has attained the compressive strength at the age of 28 days as 63.56 MPa which is increased by 10.5% than that of plain concrete. This may be attributed to the greater reduction of the amount of weak transition zone and strongly influenced by the inclusion of hybrid fibers also.

Plain concrete prisms were broken into two pieces at maximum load (sudden failure) whereas HYFECC prisms were held together after first cracking load and even at the maximum load which shows the enhancement in displacement of the beam.

3.2 Static analysis of RC beams

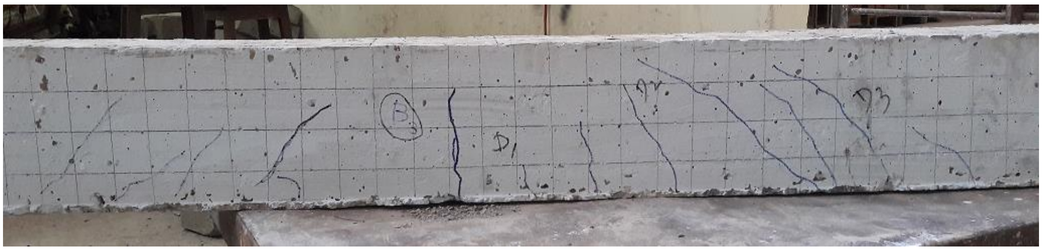

(a) Control RC beam at damage degree D_3

(b) HYFRC beam at damage degree D_3

Fig. 11 Failure patterns of RC and HYFRC beams at different damage levels

Table 6 Natural frequency values of control RC beam (ω)

Damage degree	Load (kN)	f_1 (Hz)	$\Delta f_1/f_1$ (%)	f_2 (Hz)	$\Delta f_2/f_2$ (%)	f_3 (Hz)	$\Delta f_3/f_3$ (%)	f_4 (Hz)	$\Delta f_4/f_4$ (%)	f_5 (Hz)	$\Delta f_5/f_5$ (%)	f_6 (Hz)	$\Delta f_6/f_6$ (%)
D_0	0	236.6	-	614.3	-	1120	-	1708	-	2348	-	3008	-
D_1	104.25	222.7	-5.87	583	-5.09	1073	-4.19	1638	-4.09	2260	-3.74	2895	-3.75
D_2	145.95	209.4	-5.84	554.2	-4.93	1025	-4.47	1568	-4.27	2140	-5.31	2648	-8.53
D_3	187.95	191.8	-8.40	533.6	-3.71	996.7	-2.76	1458	-7.01	2027	-5.28	2546	-3.85

Table 7 Damping ratio values of control RC beam (ζ)

Damage degree	Load (kN)	Mode 1	Mode 2	Mode 3	Mode 4	Mode 5	Mode 6
D_0	0	0.82	0.49	0.44	0.36	0.32	0.31
D_1	104.25	0.84	0.52	0.49	0.39	0.36	0.34
D_2	145.95	0.85	0.57	0.50	0.41	0.39	0.37
D_3	187.95	0.88	0.60	0.53	0.44	0.41	0.40

Beams B_1 and B_2 were control reinforced concrete beams which have been subjected to monotonic bending test and flexural vibrations in undamaged and damaged state, respectively. All RC beams and HYFRC beams were examined under complete bending failure for static analysis and partially bending loading increasing damage from D_0 to D_3.

Experimental results of static test for both RC and HYFRC beams are tabulated in Table 5. All beams were subjected to monotonic static load at two points in the mid-span equal to 400 mm and the typical view of static load test setup is shown in Fig. 9. From the figure, it can be seen that, the specimen was instrumented with three dial gauges at mid-point and loading points to evaluate the deflection of the beam while testing. All beams were white washed and girds were marked on two sides of the beam of size 50 mm×50 mm for the purpose of locating the progression of cracks. Fig. 10 shows the load versus mid-span deflection behavior of RC control and HYFRC beams. From the figure, it can be seen that, in the elastic region, the applied load was very low and the deflection of the beam was also less.

Subsequently, there was an extrinsic decrease in the stiffness of the beam due to the formation of hair-line cracks in the tension zone and the load at this point was 70 kN and 92 kN for the beams B_1 and P_1, respectively. As the load increased, crack propagates on the sides of the beam and the beam sustained more load at constant stiffness and more cracks progress towards the tension zone and hair-line cracks were formed in the compression zone under the load points. Exclusively in the tension zone cracks wereinitiated with increase of loading towards the neutral axis and the crack widens and propagates for controlled reinforced concrete beams. Furthermore, the cracked portion was effective in resisting the bending stress and bending moment, the load carrying capacity coincides with the yielding of steel. Eventually, crack enlarges more in the tension zone than the compression zone after complete yielding of reinforcement.

Fig. 11, shows the failure patterns of control RC and HYFRC beams under monotonic loading condition. Beams B_1 and P_1 have been failed in flexure at ultimate loads of 208.5 kN and 248 kN with the maximum deflection of 52 mm and 56 mm, respectively.

3.3 Flexural vibration analysis of RC beams

The beams B_2 and P_2 have been analyzed by dynamic tests to measure the dynamic characteristics at different state of damaged as well as undamaged levels. For all beams, dynamic tests have been conducted through non-destructive technique method as impact hammer technique at the end of each degree of damage as D_1, D_2 and D_3 in

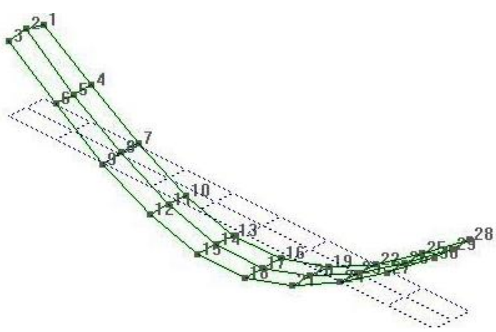

(a) First mode shape

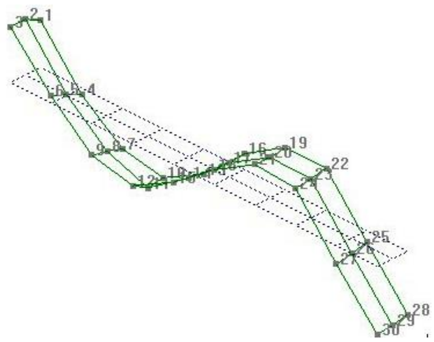

(b) Second mode shape

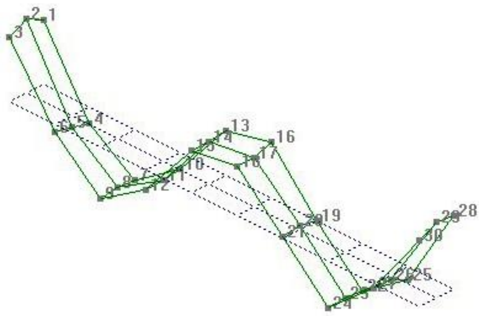

(c) Third mode shape

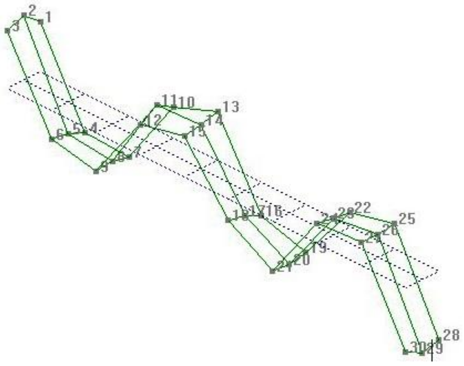

(d) Fourth mode shape

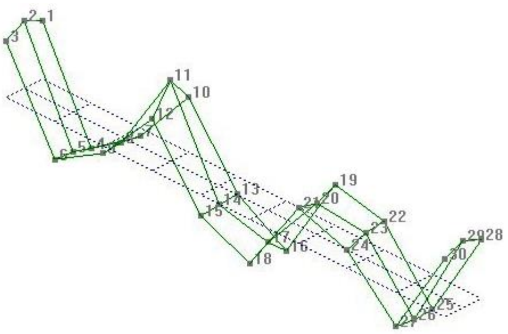

(e) Fifth mode shape

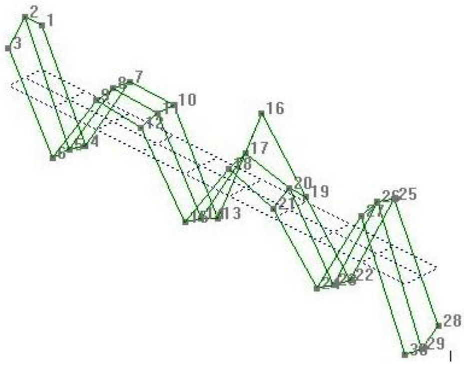

(f) Sixth mode shape

Fig. 12 Typical view of mode shapes at different vibration levels

free-free constraints.

Dynamic parameters such as natural frequency, damping ratio and mode shapes have been obtained for all specimens through experimental flexural vibration results. Experimental natural frequency and damping ratio values of control RC beam (B_2) are illustrated in Table 6 and Table 7, respectively. The aforementioned beam has been analyzed by dynamic test at undamaged level (D_0) which was followed by static and dynamic tests at the end of each damage levels from D_1, D_2 and D_3 as 50%, 70% and 90% of ultimate load, respectively which has been taken from beam B_1. From the obtained dynamic results, the natural frequency decreases with the increase of damage whereas the damping ratio increases with the increase in structural damage of the beam.

Fig. 12 displays the mode shapes of reinforced concrete beams arbitrarily. The envelope of frequency response functions (FRFs) are shown in Fig. 13 for control RC beam at undamaged state, which has been obtained by dynamic test in the frequency range of 0-4000Hz. Generally, the form of the FRFs used in the experimental technique is inertance which returns a measure of the amplitude in terms

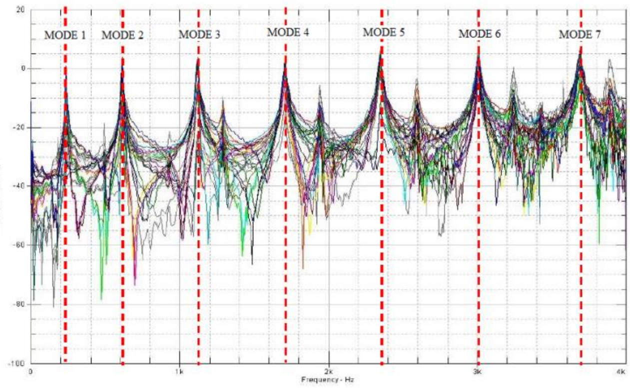

Fig. 13 Envelope of FRFs at undamaged (D_0) state for control RC beam

Table 8 Natural frequency values of HYFRC beam (ω)

Damage degree	Load (kN)	f_1 (Hz)	$\Delta f_1/f_1$ (%)	f_2 (Hz)	$\Delta f_2/f_2$ (%)	f_3 (Hz)	$\Delta f_3/f_3$ (%)	f_4 (Hz)	$\Delta f_4/f_4$ (%)	f_5 (Hz)	$\Delta f_5/f_5$ (%)	f_6 (Hz)	$\Delta f_6/f_6$ (%)
D_0	0	239.5	-	627	-	1136	-	1732	-	2363	-	3036	-
D_1	124	217	-9.39	596.3	-4.89	1089	-4.13	1666	-3.81	2276	-3.68	2929	-3.52
D_2	173.6	209.8	-3.31	578	-3.06	1067	-2.02	1609	-3.42	2198	-3.42	2851	-2.66
D_3	223.2	200.6	-4.38	557.9	-3.47	1023	-4.12	1540	-4.28	2104	-4.27	2701	-5.26

Table 9 Damping ratio values of HYFRC beam (ζ)

Damage degree	Load (kN)	Mode 1	Mode 2	Mode 3	Mode 4	Mode 5	Mode 6
D_0	0	0.87	0.59	0.49	0.38	0.34	0.30
D_1	124	0.92	0.62	0.51	0.41	0.37	0.33
D_2	173.6	0.95	0.64	0.53	0.44	0.40	0.35
D_3	223.2	0.98	0.67	0.54	0.46	0.41	0.38

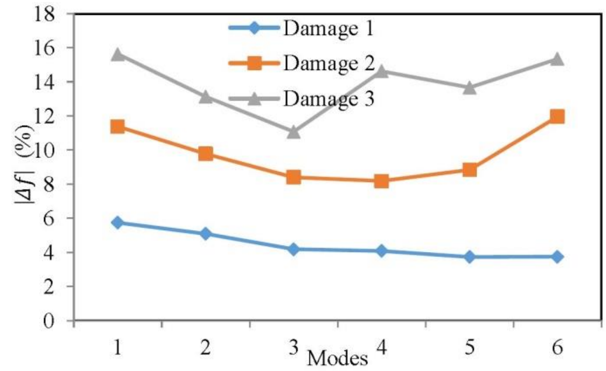

Fig. 14 Comparison of natural frequencies at different damage levels for control RC beam

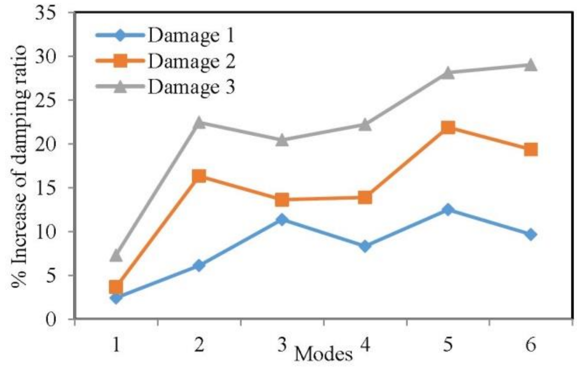

Fig. 15 Comparison of damping ratios at different damage levels for control RC beam

of acceleration starting from random excitations through the Fast Fourier Transform (FFT) method.

Comparison of experimental natural frequencies and damping ratios of control RC beam with undamaged level are shown in Fig. 14 and Fig. 15, respectively for six vibration modes. Similar dynamic response technique has been used to analyze the HYFRC beams P_2 at each damage levels. Natural frequency and damping ratio values for HYFRC beams P_2 are tabulated in Tables 8 and 9, respectively. Figs. 16 and 17 contain the comparison of the natural frequencies and damping ratios with undamaged state for beam P_2, respectively for six modes of vibration.

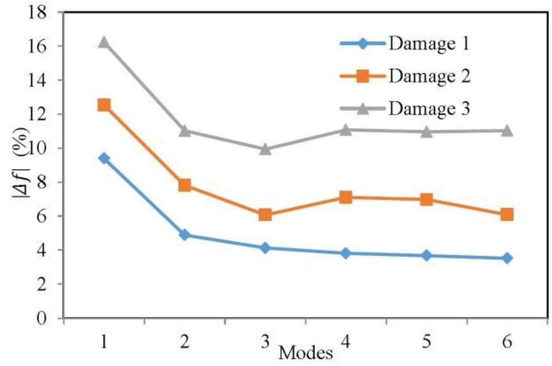

Fig. 16 Comparison of natural frequencies at different damage levels for HYFRC beam

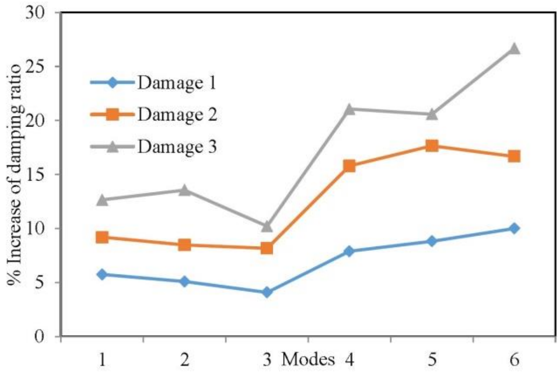

Fig. 17 Comparison of damping ratios at different dam age levels for HYFRC beam

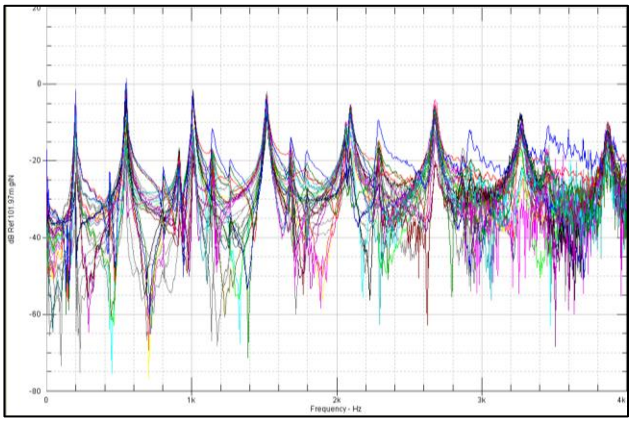

Fig. 18 Envelope of FRFs at second damage degree (D_2) for HYFRC beam

The experimental FRF diagrams at different damage levels for HYFRC beam is shown in Fig. 18. Eventually, moment ratio versus frequency variation ratio for beams B_2 and P_2 at each damage levels with six vibration modes are shown in

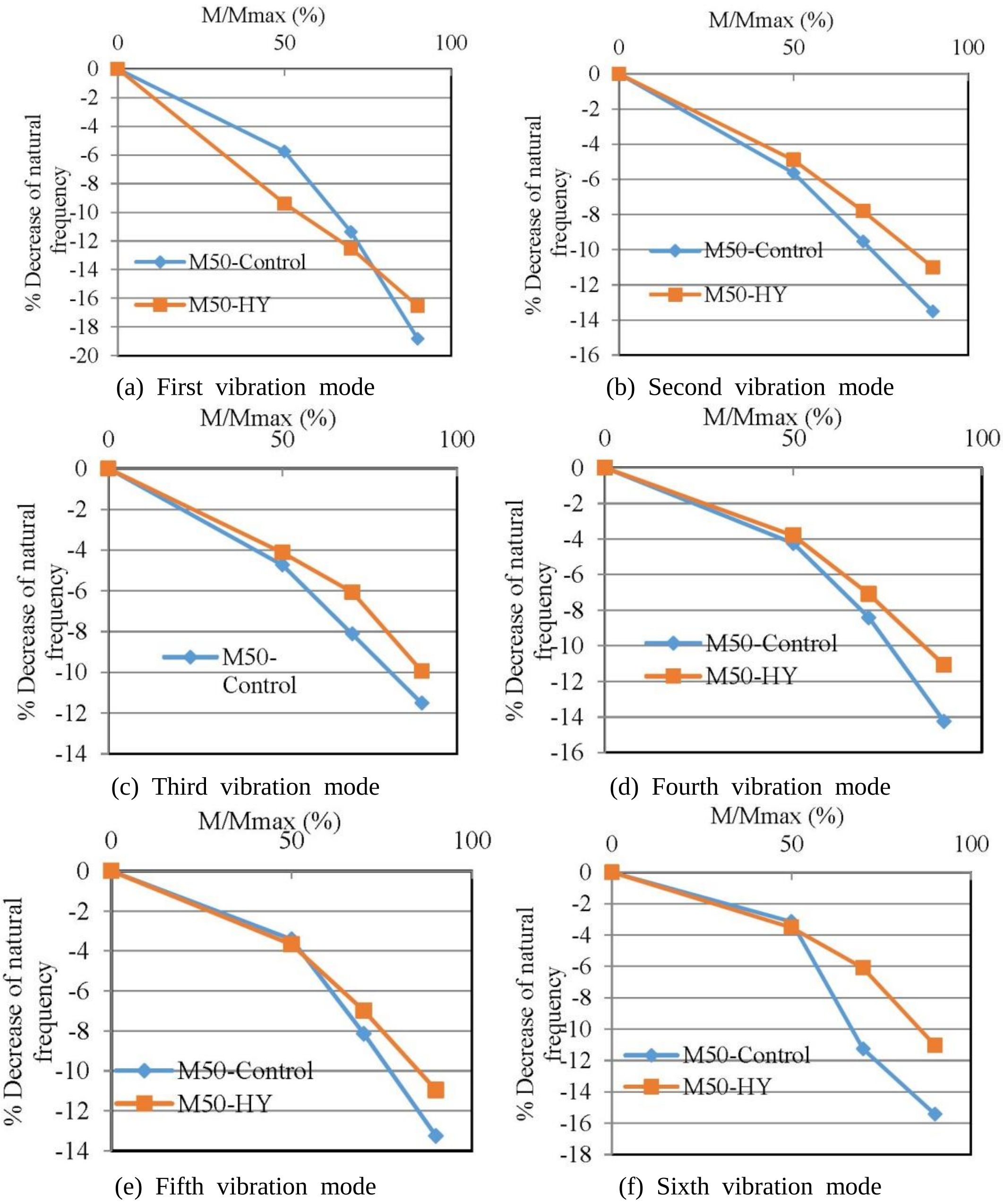

Fig. 19 Comparison of M/Mmax ratios Vs. frequency ratios for RC and HYFRC beams

Fig. 19. From the figure, it can be observed that, a rapid decrease of natural frequency values in the case of increase of damage degrees. Fig. 20 displays the P/P_{max} ratio versus damping ratios of RC and HYFRC beams for undamaged as well as each damage degree levels for all six vibration modes. From the figure, it can be observed that the damping values increased with the increase of damage degrees.

4. Conclusions

In this experimental investigation, static and dynamic behavior of HYFRCs was studied and compared with control RC beams. From the experimental results, the following conclusions can be drawn,

- The content of fibers combined with steel and polypropylene concrete mixtures, resulted in enhanced behavior in terms of overall performance of static properties accompanied by compressive, splitting tensile and flexural strength.
- Flexural strength increased with the addition of both steel-PP hybrid fibers when compared to control concrete and also it enhances the post-cracking behavior of concretes. The flexural strength increased by about 64% when compared with non-fibrous concrete.
- The gain in splitting tensile strength has been improved depending upon the addition of total volume fraction of hybrid fibers as well as the individual fiber content. The increase in concrete splitting tensile strength at the age of 28 days for the total volume fraction of 0.5% was about 56.4% with the combination of 75-25 percentage variation of steel and PP fibers,

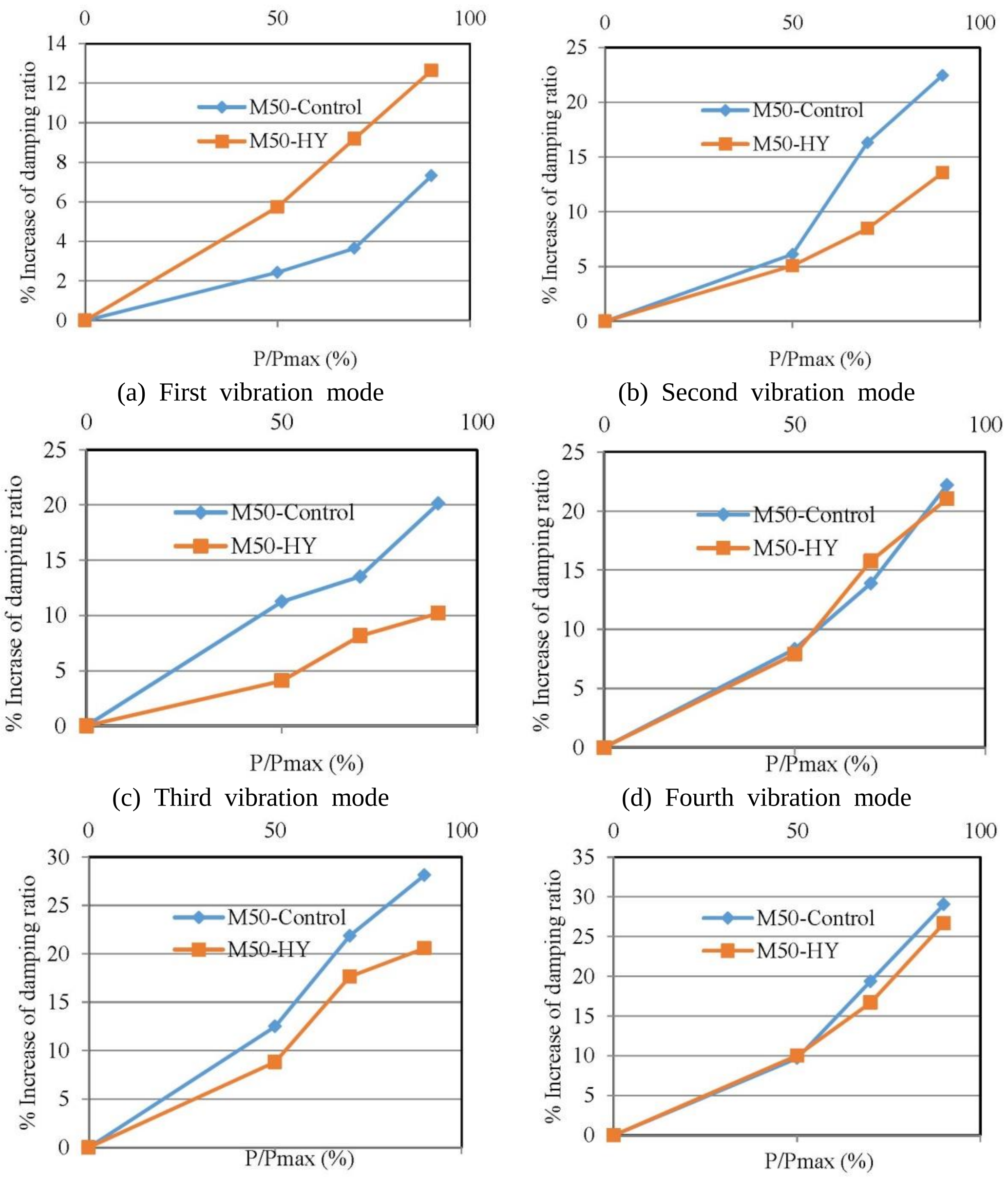

(a) First vibration mode (b) Second vibration mode

(c) Third vibration mode (d) Fourth vibration mode

(e) Fifth vibration mode (f) Sixth vibration mode

Fig. 20 Comparison of P/Pmax ratios Vs. Damping ratios for RC and HYFRC beams

respectively.

- In the static test of FGRC beams, the addition of hybrid fibers which was incorporated with steel and PP fibers were led to an increase of about 18.94% when compared with control RC beams.

- From undamaged state to damage degree D_3, the natural frequencies for both RC beam B_2 and HYFRC beam P_2 decreased by about 13.6% and 7% at fifth mode, whereas the damping ratio increased by approximately 28% and 20.5% at the same mode, respectively.

- Finally, the vibration based monitoring technique is one of the best methods which used to assess the damage analysis of reinforced concrete beams and it could be correlated to the loading degrees also. Changes from un-cracked to cracked sections were recorded by decreasing of natural frequency values.

References

10262 (2009), Guidelines for Concrete Mix Proportioning.

Alberti, M.G., Enfedaque, A. and Galvez, J.C. (2014), "On the mechanical properties and fracture behavior of polyolefin fiber reinforced self-compacting concrete", *Constr. Build. Mater.*, **55**, 274-288. https://doi.org/10.1016/j.conbuildmat.2014.01.024.

Alberti, M.G., Enfedaque, A. and Galvez, J.C. (2014), "Polyolefin fiber-reinforced concrete enhanced with steel-hooked fibers in low proportions", *Mater. Des.*, **60**, 57-65. https://doi.org/10.1016/j.matdes.2014.03.050.

ASTM C78-94, Standard Test Method for Flexural Strength of Concrete.

Barros, J.A.O. and Dias, S.J.E. (2006), "Near surface mounted CFRP laminates for shear strengthening of concrete beams", *Cement Concrete Compos.*, **28**(3), 276-292. https://doi.org/10.1016/j.cemconcomp.2005.11.003.

Brandt, A.M. (2008) "Fiber reinforced cement-based (FRC)

Composites after over 40 years of development in building and civil engineering", *Compos. Struct.*, **83**(3), 3-9. https://doi.org/10.1016/j.compstruct.2008.03.006.

Caleb, C.W., Li, H.C.H. and Whittingham, B. (2009), "Damage detection in repairs using frequency response technique", *Compos. Struct.*, **87**, 175-180. https://doi.org/10.1016/j.compstruct.2008.05.010.

Capozucca, R. (2009), "Static and dynamic response of damaged RC beams strengthened with NSM CFRP rods", *Compos. Struct.*, **91**, 237-248. https://doi.org/10.1016/j.compstruct.2009.05.003.

Capozucca, R. (2013), "A reflection on the application of vibration tests for the assessment of cracking in PRC/RC beams", *Eng. Struct.*, **48**, 508-518. https://doi.org/10.1016/j.engstruct.2012.09.022.

Capozucca, R. (2018), "Vibration analysis of damaged RC beams strengthened with GFRP", *Compos. Struct.*, **200**, 624-634. https://doi.org/10.1016/j.compstruct.2018.05.112.

Capozucca, R., Domizi, J. and Magagnini, E. (2016), "Damaged RC beams strengthened with NSM CFRP rectangular rods under vibration in different constrain conditions", *Compos. Struct.*, **154**, 660-683. https://doi.org/10.1016/j.compstruct.2016.07.044.

Chaohua, J., Ke, F. and Da, C. (2014) "Experimental study on the mechanical properties and microstructure of chopped basalt fiber reinforced concrete", *Mater. Des.*, **58**, 187-193. https://doi.org/10.1016/j.matdes.2014.01.056.

Constatine, E.C., Chris, G.K., Georgia, M.A., Nikos, A.P., Maria, J.F. and Costas, P.P. (2016), "Applications of smart piezoelectric materials in a wireless admittance monitoring system (WiAMS) to structures-Tests in RC beams", *Case Stud. Constr. Mater.*, **5**, 1-18. https://doi.org/10.1016/j.cscm.2016.03.003.

Dawood, E.T. and Ramli, M. (2010), "Development of high strength flowable mortar with hybrid fiber", *Constr. Build. Mater.*, **6**, 1043-1050. https://doi.org/10.1016/j.conbuildmat.2010.11.008.

Di Prisco, M., Lamperti, T. and Lapolla, S. (2008), "HPFRCC thin plates for precast roofing", *Procedings of the Second International Symposium on Ultra-high Performance Concrete*.

Filip, G., Michal, M. and Tomasz, T. (2019), "Mechanical properties of fiber reinforced concrete with recycled fibers", *Constr. Build. Mater.*, **198**, 323-331. https://doi.org/10.1016/j.conbuildmat.2018.11.183.

Ganesan, N., Indira, P.V. and Himasree, P.R. (2018), "Strength and behavior of bamboo reinforced concrete wall panels under two way in-plane section", *Adv. Concrete Constr.*, **6**(1), 1-13. https://doi.org/10.12989/acc.2018.6.1.001.

Hamed, A., Iman, M.N., Saman, R.R. and Ahmed, A. (2018), "Experimental measurement of dynamic properties of composite slabs from frequency response", *Measure.*, **114**, 150-161. https://doi.org/10.1016/j.measurement.2017.09.030.

Huang, X., Ma, G.W. and Li, J.C. (2010), "Damage assessment of reinforced concrete structural elements subjected to blast load", *Int. J. Protect. Struct.*, **1**(1), 103-124. https://doi.org/10.1260/2041-4196.1.1.103.

Huszav, Z. (2008), "Vibrations of cracked reinforced and pre-stressed concrete beams", *Arch. Civil Mech. Eng.*, **6**(2), 155-164. https://doi.org/10.2298/FUACE0802155H.

IS 12269 (1987), Indian Standard Specification for 53 Grade Ordinary Portland Cement.

IS 383 (1999), Indian Standard Specification for Coarse and Fine Aggregates from Natural Source for Concrete.

Kim, D.J., Park, S.H. and Ryu, G.S. (2011), "Comparative flexural behavior of hybrid ultra-high performance FRC with different micro fibers", *Constr. Build. Mater.*, **25**(11), 4144-4155. https://doi.org/10.1016/j.conbuildmat.2011.04.051.

Lim, J.C. and Ozbakkaloglu, T. (2014), "Influence of silica fume on stress-strain behavior of FRP confined HSC", *Constr. Build. Mater.*, **63**, 11-24. https://doi.org/10.1016/j.conbuildmat.2014.03.044.

Muntean, R., Cazacu, C. and Mizgan, P. (2017), "Practical applications of dispersely reinforce concrete with polypropylene fibers", *Procedia Eng.*, **181**, 285-292.

Naaman, A.E. and Reinhardt, H.W. (2006), "Proposed classification of HPFRC composites based on their tensile response", *Mater. Struct.*, **39**(5), 547-555. https://doi.org/10.1617/s11527-006-9103-2.

Shahiron, S., Rhys, P., Norazura, M.B. and Karen, M.H. (2013), "Damage classification of reinforced concrete beam by acoustic emission signal analysis", *Constr. Build. Mater.*, **45**, 78-86. https://doi.org/10.1016/j.conbuildmat.2013.03.095.

Shaikh, F.U.A. and Taweel, M. (2015), "Compressive strength and flexural behavior of fiber reinforced concrete at elevated temperature", *Adv. Concrete Constr.*, **3**(4), 283-293. https://doi.org/10.12989/acc.2015.3.4.283.

Tiberti, G., Minelli, F. and Plizzari, G.A. (2014), "Influence of concrete strength on crack development of SFRC members", *Cement Concrete Compos.*, **45**, 176-185. https://doi.org/10.1016/j.cemconcomp.2013.10.004.

Yang, K.H. (2011), "Tests on concrete reinforced with hybrid or monolithic steel and polyvinyl alcohol fibers", *ACI Mater. J.*, **108**(6), 664-672.

Yao, W., Li, J. and Wu, K. (2003), "Mechanical properties of hybrid fibers-RC a low fiber volume fraction", *Cement Concrete Res.*, **33**(1), 27-30. https://doi.org/10.1016/S0008-8846(02)00913-4.

CC